TIME-FREQUENCY APPROXIMATION AND FEATURE EXTRACTION FOR RANGE-DEPENDENT UNDERWATER SOUND PROPAGATION

by

Vikram Thiruneermalai Gomatam

B.E. Electronics and Communication, Visvesvaraya Technological University,

2007

Submitted to the Graduate Faculty of

the Swanson School of Engineering in partial fulfillment

of the requirements for the degree of

Master of Science

University of Pittsburgh

2011

UNIVERSITY OF PITTSBURGH

SWANSON SCHOOL OF ENGINEERING

This thesis was presented

by

Vikram Thiruneermalai Gomatam

It was defended on

July 12, 2011

and approved by

Patrick J. Loughlin, PhD, Professor, Depts. of Bioengineering and Electrical and Computer Engineering

Amro El-Jaroudi, PhD, Associate Professor, Dept. of Electrical and Computer Engineering

Zhi-Hong Mao, PhD, Assistant Professor, Dept. of Electrical and Computer Engineering

Thesis Advisor: Patrick J. Loughlin, PhD, Professor, Depts. of Bioengineering and Electrical and Computer Engineering

TIME-FREQUENCY APPROXIMATION AND FEATURE EXTRACTION FOR RANGE-DEPENDENT UNDERWATER SOUND PROPAGATION

Vikram Thiruneermalai Gomatam, M.S.

University of Pittsburgh, 2011

Sonar systems are used in localization, detection and classification of various objects in marine environments. Unlike the propagation of sound in air, which is largely unaffected by dispersion, the underwater channel can be highly dispersive, especially in shallow water environments. Such channels also introduce other significant propagation effects, including multipath and frequency-dependent energy attenuation due to interactions of the sound with the ocean surface and bottom. Compensating for these propagation effects is important with regard to classification of underwater objects based on their sonar backscatter, as the target signature will be different at different locations. Previous work in our lab has developed feature extraction methods for dispersion-invariant classification, and approximation methods to solve for dispersive propagation, in range-independent environments. Such environments, wherein the channel characteristics do not change with propagation distance, represent an idealistic assumption that generally does not hold for long-range propagation in underwater channels.

In this work we concentrate on range-dependent guided wave propagation. We begin with an examination of the classification performance of the previously developed range-independent features in a range-dependent model, namely an ideal wedge waveguide. Motivated by the degradation in classification performance of these features, we derive new features that mitigate the range-dependent dispersion effects and show that the derived features outperform range-independent features in a wedge waveguide. We also derive the approximate Wigner distribution for a pulse propagating in this range-dependent environ-

ment, and highlight similarities and differences of this new result with a previously developed range-independent approximation. This approximation can be a useful tool for estimating the evolution of pulse propagating in a range-dependent channel.

Finally, we explore a second range-dependent model, namely the Parabolic Equation, which can be adapted to a wide array of propagation environments and media. We derive features that are invariant to dispersion and attenuation from this model.

TABLE OF CONTENTS

LIST OF TABLES

LIST OF FIGURES

1.0 INTRODUCTION

Classification and detection of objects based on their backscattered sonar signatures is complicated due to the propagation effects induced by the channel, the effects of frequency dependent dispersion and attenuation being the most prominent in shallow waters. In order for us to improve the classification performance, we have to come up with methods that negate the effects introduced by the channel.

It has been well documented by Okopat et al., [1, 11] that the propagation effects can be better characterized in time-fequency domain and consequently they developed a phase space propagation model based on the Wigner distribution. The model was then used to develop propagation-invariant features and characterize the statistical nature of ordinary moment features. The features derived were the ADIMS (attenuation- and dispersion-invariant moments) [13], and its offshoot the Cepstral moments (CMOM) that showed invariance to a dispersive and absorptive channel and dispersion only channel, respectively.

In our work we apply a range-dependent propagation model based on the WKB approximation for the adiabatic mode theory. We simulate a specific case of the range dependent model (the ideal wedge), commonly seen in littoral environments. We then apply the feature extraction process derived by Okopal et al., [1, 11] for backscatter propagated in the wedge environment to assess classification performance. We show that as the slope of the bottom gets steeper the performance of the features degrades, as anticipated given that the features derived were under the assumption that the propagation is range-independent.

This led us to derive features specific to the wedge environment which we call the Range-Dependent Dispersion Invariant Moments (RDIMS) based on the adiabatic mode theory model previously used to simulate the wedge waveguide. The RDIMS are invariant to range-dependent dispersion, but not absorption.

The Wigner approximation was previously developed to study the pulse evolution as it propagates in a dispersvie media. It was shown to be a useful tool to approximate the sonar pulse propagating in a realistic ocean environment (which includes dispersion and attenuation). We extend that concept to the adiabatic range-dependent model and show that the resulting expression, while different, retains a similar form to the range-independent case.

Finally, we take a look at the parabolic(PE) model which overcomes the limitations posed by the adiabatic and the normal mode theory and can practically be applied to any environment. We theoretically derive invariant moments based on this model. We then summarize our work and suggest a few possible avenues that could be explored in the near future.

2.0 THE RANGE DEPENDENT PROPAGATION

2.1 INTRODUCTION

This chapter summarizess the previous work that is relevant to our investigation. We first look at the formulation of the wave equation and solution for range independent propagation. A short treatment about the range independent moments derived previously is also made. The extension of the Normal-Mode solution to the range dependent environment is discussed. We take an in depth look at the adiabatic mode theory, achieved by the WKB approximation of the standard Helmholtz equation. We then simulate the ideal wedge using that model. The range independent moments are then evaluated for the backscatter propagating in an ideal wedge and comments about their classification performance are made.

2.2 BACKGROUND

2.2.1 The Wave Equation

The acoustic wave equation has its starting point from the standard Helmholtz equation for a more complete treatment the reader is referred to [18],

$$\nabla^2 p = \frac{1}{c^2}\frac{\partial^2 p}{\partial t^2} \tag{2.1}$$

where p is the wave and c is the underwater sound speed. The term ∇ is del, the co-ordinate specific differential operator. Expanding del for rectangular co-ordinates we obtain,

$$\frac{\partial^2 p}{\partial x^2} + \frac{\partial^2 p}{\partial y^2} + \frac{\partial^2 p}{\partial z^2} = \frac{1}{c^2}\frac{\partial^2 p}{\partial t^2} \tag{2.2}$$

For the sake of simplicity and to facilitate the application of the model in a realistic ocean environment, we assume an infinite line source along the y-axis thereby reducing the problem to that of plane wave propagation. Our objective is to now solve for the remaining x and z co-ordinates.

The wave is exponentially time dependent (i.e. $p(x,z,t) = p(x,z)e^{-j\omega t}$) and the above equation is co-ordinate separable $p(x,z) = \varphi(x)\psi(z)$. Then Eq. (2.2) becomes

$$\frac{d^2\varphi(x)}{dx^2}\psi(z) + \frac{d^2\psi(z)}{dz^2}\varphi(x) + \frac{\omega^2}{c^2}\varphi(x)\psi(z) = 0 \tag{2.3}$$

where z is depth and x is the range coordinate. Separating variables we have,

$$\frac{d^2\psi(z)}{dz^2} + k_z^2\psi(z) = 0 \tag{2.4}$$

$$\frac{d^2\varphi(x)}{dx^2} + (\frac{\omega^2}{c^2} - k_z^2)\varphi(x) = 0 \tag{2.5}$$

The solution to Eq. (2.4) is

$$\psi(z) = A\sin(k_z z) \tag{2.6}$$

under the assumption that the field vanishes at the boundaries, i.e. $\psi(0) = \psi(z_0) = 0$, where $z = z_0$ is the depth of the ocean channel (i.e. the plate separation for a paralle-plate waveguide), for which we have

$$k_z = \frac{m\pi}{z_0} \tag{2.7}$$

where $m = 1, 2, ...$ is the mode number.

The Solution to Eq. (2.5) is

$$\varphi(x) = e^{jk_x x} \tag{2.8}$$

where

$$k_x = \sqrt{(\frac{\omega}{c})^2 - k_z^2} = \sqrt{(\frac{\omega}{c})^2 - (\frac{m\pi}{z_0})^2} \tag{2.9}$$

the solution $\varphi(x)$ represents the propagating (outgoing) component of the wave. This form of solution is called the Normal-mode solution to the wave equation. Henceforth, we will consider the propagation per mode (often m=1) unless noted otherwise. A more detailed treatment on the Normal-Mode theory is available in [18, 6, 11].

In this solution we can see that the boundary remains constant (i.e. the field terminates at the same z for all x). These belong to the class of range independent waveguides. The physical significance being that the dispersion factor Eq. (2.9) remains constant for all x. In reality, there are few real world scenarios that fall under the range-independent propagation model.

2.2.2 The Range-Independent Moments

Exploiting the properties of range independent propagation given in Eq. (2.8), several invariant features for classification were developed as summarized below [13]:

Let the wave at $x = 0$ be written as $u(0, t)$. The spectrum of the wave can be written as $F(0, \omega)$. The Fourier transform at position x and its dual can be written as [14]

$$u(x, t) = \frac{1}{\sqrt{2\pi}} \int F(0, \omega) e^{jk_x(\omega)x} e^{-j\omega t} d\omega \tag{2.10}$$

where $k_x(\omega)$ is given in Eq. (2.9), and

$$F(0, \omega) = \frac{1}{\sqrt{2\pi}} \int u(0, t) e^{j\omega t} d\omega \tag{2.11}$$

$$F(x, \omega) = F(0, \omega) e^{jk_x(\omega)x} \tag{2.12}$$

and

$$k_x(\omega) = k_{Rx}(\omega) + jk_{Ix}(\omega) \tag{2.13}$$

where k_{Rx} and k_{Ix} are the real and imaginary parts of the dispersion relation. The spectrum of the signal can also be expressed in terms of its amplitude and phase components,

$$F(x,\omega) = B(x,\omega)e^{j\psi(x,\omega)} \tag{2.14}$$

Upon equating the magnitude and the phase components we obtain,

$$B(x,\omega) = B(0,\omega)e^{-k_I(\omega)x} \tag{2.15}$$

$$\psi(x,\omega) = \psi(0,\omega) + k_R(\omega)x \tag{2.16}$$

and where $B(0,\omega)$ and $\psi(0,\omega)$ are the magnitude and phase spectrum of the initial signal.

The phase space form shown above can be used to derive features shown in the subsequent sections.

2.2.2.1 Attenuation and Dispersion Invariant Moments (ADIMs) The absorption of sound in water is frequency dependent and is power-law in nature, Eq. (2.13), for which the imaginary part of the dispersion relation is $k_{Ix}(\omega) = \beta\omega$ where β is the absorption coefficient which normally is $10^{-8}m^{-1}Hz^{-1}$ for ocean water.

Substituting this in to Eq. (2.15) we get,

$$B(x,\omega) = B(0,\omega)e^{-\beta\omega x} \tag{2.17}$$

Taking the natual log on both sides yields

$$\ln B(x,\omega) = \ln B(0,\omega) - \beta\omega x \tag{2.18}$$

Then, let,

$$Z(x,\omega) = \frac{\partial}{\partial\omega}\ln B(x,\omega) = \frac{B'(x,\omega)}{B(x,\omega)} = \frac{B'(0,\omega)}{B(0,\omega)} - \beta x \tag{2.19}$$

Now the βx term is reduced to a level shift which can be eliminated by taking the mean over frequency,

$$Z_0(x,\omega) = Z(x,\omega) - \overline{Z(x,\omega)} \tag{2.20}$$

where

$$\overline{Z(x,\omega)} = \int Z(x,\omega) d\omega \tag{2.21}$$

The spectral function $Z_0(x,\omega)$ is now invariant to dispersion and absorption. To compute temporal moments we do the inverse Fourier transform of Eq. (2.20).

$$v(x,t) = \frac{1}{\sqrt{2\pi}} \int \exp(Z_0(x,\omega)) e^{-j\omega t} d\omega \tag{2.22}$$

$$T_x(x) = \int t^n \left| v(x,t) \right|^2 dt \tag{2.23}$$

This feature is now independent of propagation effects and its moments can be used for object classification.

2.2.2.2 Cepstral Moments The Cepstral moments are similar in theme to the ADIMS [12]. For a signal $u(x,t)$ the cepstrum is written as

$$c_u(x,t) = \frac{1}{\sqrt{2\pi}} \int \ln \left| B(x,\omega) \right| e^{-j\omega t} d\omega \tag{2.24}$$

It is evident that if the dispersion is not complex Eq. (2.15), the cepstrum is invariant to dispersion and the temporal moments of the cepstrum are computed as

$$M_c(x;n) = \int t^n \left| c_u(x,t) \right|^2 dt \tag{2.25}$$

2.3 RANGE DEPENDENT PROPAGATION

A significant amount of transverse wave propagation occurs in the shallow water continental shelf region which can be approximated to an ideal wedge. The wedge is range-dependent in nature as the boundaries change with propagation. There are many methods to solve the range-dependent propagation using the framework of the standard modal solution format, viz. the coupled mode, the adiabatic mode and the intrinsic mode.

2.3.1 Line source in Plane Geometry

In this work we use the adiabatic approximation. The solution is derived under the assumption that there is no coupling between modes(i.e. the modes are "adiabatic" in nature [19]). The argument for their usage in our work being that the end solution we obtain is similar in structure to what we had in the range-independent case and since invariant features have been extracted from the range-independent model before, a model similar to that would also be conducive for feature extraction. In addition, the adiabatic mode theory yields a solution that is simpler when compared with other range dependent models. However, the adiabatic approximation has certain limitations like it holds only for cases where the variation of depth is small compared to the variation of range and the environment shouldn't have any sudden changes in the boundaries or obstructions; such environments are often referred to as weakly-range-dependent environment.

The starting point is again the Helmholtz equation in rectangular co-ordinates

$$\frac{\partial^2 p}{\partial x^2} + \frac{\partial^2 p}{\partial y^2} + \frac{\partial^2 p}{\partial z^2} = \frac{1}{c^2}\frac{\partial^2 p}{\partial t^2} \tag{2.26}$$

We assume an infinite line source thereby eliminating the y co-ordinate out of the standard equation.

$$\frac{\partial^2 p}{\partial x^2} + \frac{\partial^2 p}{\partial z^2} = \frac{1}{c^2}\frac{\partial^2 p}{\partial t^2} \tag{2.27}$$

The assumed wave p has exponential dependence on time as well. Hence we rewrite it as $p = pe^{-j\omega t}$(keeping the notation for the signal the same).

Thus the previous equation reduces to

$$\frac{\partial^2 p}{\partial x^2} + \frac{\partial^2 p}{\partial z^2} = -\frac{\omega^2}{c^2} p \tag{2.28}$$

$$\frac{\partial^2 p}{\partial x^2} + \frac{\partial^2 p}{\partial z^2} + \frac{\omega^2}{c^2} p = 0 \tag{2.29}$$

As before, we shall use the seperation of variables technique to find a solution for the above equation. We need a solution of the form $p(x, z) = \varphi(x)\psi(z)$. The above equation then reduces to

$$\frac{d^2\varphi(x)}{dx^2}\psi(z) + \frac{d^2\psi(z)}{dz^2}\varphi(x) + \frac{\omega^2}{c^2}\varphi(x)\psi(z) = 0 \tag{2.30}$$

Separating the individual variables

$$\frac{d^2\psi(z)}{dz^2} + k_z^2\psi(z) = 0 \tag{2.31}$$

$$\frac{d^2\varphi(x)}{dx^2} + (\frac{\omega^2}{c^2} - k_z^2)\varphi(x) = 0 \tag{2.32}$$

Following in the vein of Eqs. (2.5), (2.9), we define

$$k_x = \sqrt{(\frac{\omega^2}{c^2} - k_z^2)} \tag{2.33}$$

As Eq. (2.31) is of the form $\psi''(z) + k_z^2\psi(z) = 0$, the solution to the depth co-ordinate is

$$\psi(z) = A\sin(k_z z) \tag{2.34}$$

Now, since the depth is range-dependent we have, by the vanishing boundary condition at $z = f(x)$,

$$k_z = \frac{m\pi}{f(x)} \tag{2.35}$$

Substitute in Eq. (2.33) we get the following expression.

$$k_x(x) = \sqrt{(\frac{\omega^2}{c^2} - (\frac{m\pi}{f(x)})^2)} \tag{2.36}$$

Modifying the depth separated equation for the range dependent case

$$\frac{d^2\varphi(x)}{dx^2} + k_x^2(x)\varphi(x) = 0 \tag{2.37}$$

Now, to solve this more complex differential equation, we assume a solution with a range dependent amplitude component and a range dependent phase (a standard solution for second order unforced wave equation), i.e.,

$$\varphi(x) = A(x)e^{j\phi(x)} \tag{2.38}$$

Plugging this into Eq. (2.36) yields

$$A''(x)e^{j\phi(x)} + 2jA'(x)\phi'(x)e^{j\phi(x)} + jA(x)\phi''(x)e^{j\phi(x)} - A(x)\phi'^2(x)e^{j\phi(x)} + k_x^2(x)A(x)e^{j\phi(x)} = 0 \tag{2.39}$$

Factoring out the $e^{j\phi(x)}$ and then separating the remaining factor into real and imaginary parts yields

Real Part:

$$A''(x)e^{j\phi(x)} + A(x)\left[k_x^2(x) - \phi'^2(x)\right] = 0 \tag{2.40}$$

Imaginary Part:

$$2A'(x)\phi'(x) + A(x)\phi''(x) = 0 \tag{2.41}$$

We now introduce the WKB approximation [17] to Eq. (2.40), which holds under the condition that there is only a small variation in the envelope $A(x)$ compared to the variation in range x: 'weak' range dependence condition. Hence, the second order differential of $A(x)$ is small and therefore negligible. Thus, the WKB approximation to Eq. (2.40) yields

$$\pm k_x(x) = \phi'(x) \tag{2.42}$$

such that

$$\phi(x) = \pm \int_{x_S}^{x_R} k_x(x)dx \tag{2.43}$$

where x_S and x_R denote the location of source and receiver, respectively. Now, plugging this result for $\varphi(x)$ into Eq. (2.41) yields

$$A(x) = \frac{B}{\sqrt{k_x(x)}} \tag{2.44}$$

Hence, the total solution at x_R works out to,

$$\varphi(x_R; x_S) = \frac{B}{\sqrt{k_x(x_R)}} e^{\pm j \int_{x_S}^{x_R} k_x(x')dx'} \tag{2.45}$$

where 'B' is a constant derived from the standard range-independent solution which equals '1'.

This can be applied to any 'weakly' range dependent environment. For our work, we use a specific case of the weakly-range-dependent solution, i.e. the ideal wedge, where the variation of depth w.r.t range is given by

$$z = x \tan\theta \tag{2.46}$$

where θ is the angle of the wedge at its apex. The dispersion relation can now be written as

$$k_x(x) = \sqrt{(\frac{\omega^2}{c^2} - (\frac{m\pi}{x \tan\theta})^2)} \tag{2.47}$$

2.3.1.1 Analogy with range independent propagation For the sake of academic completeness we show that the WKB approximation for the range-dependent environment is analogous to the range-independent propagation. This follows on the footsteps of the previous derivation. Starting from the range co-ordinate,

$$\frac{d^2\varphi(x)}{dx^2} + k_x^2\varphi(x) = 0 \tag{2.48}$$

we assume a solution of the form

$$\varphi(x) = A(x)e^{j\phi(x)} \tag{2.49}$$

Substitute in Eq. (2.48) we obtain

$$\frac{d^2\varphi(x)}{dx^2} = A''(x)e^{j\phi(x)} + 2jA'(x)\phi'(x)e^{j\phi(x)} + jA(x)\phi''(x)e^{j\phi(x)} - A(x)\phi'^2(x)e^{j\phi(x)} \tag{2.50}$$

separating the real and imaginary parts yields

Real Part:

$$A''(x) + \left[k_x^2 - \phi'^2(x)\right] = 0 \tag{2.51}$$

Imaginary Part:

$$2A'(x)\phi'(x)e^{j\phi(x)} + A(x)\phi''(x)e^{j\phi(x)} = 0 \tag{2.52}$$

By the WKB approximation, the second order amplitude function is neglected. Hence, we have

$$\pm k_x = \phi'(x) \tag{2.53}$$

and

$$\phi(x) = \pm k_x \int_{x_S}^{x_R} dx \tag{2.54}$$

Plugging this into the imaginary part yields

$$A(x) = C \tag{2.55}$$

Thus the total solution is given by:

$$\varphi(r;s) = Ce^{\pm jk_x \int_{x_S}^{x_R} dx} \tag{2.56}$$

where 'C' is a constant. whose value is determined from the homogeneous range-independent solution equaling '1' (From Eq. (2.5)).

Total solution

$$\varphi(r;s) = e^{jk_x(x_R - x_S)} \tag{2.57}$$

2.3.2 Point Source with Azimuthal Symmetry

One interesting observation is that the adiabatic-mode solution is able to hold its validity for point sources with azimuthal symmetry.

Starting with the Helmholtz equation in cylindrical co-ordinates:

$$\frac{1}{r}\frac{\partial}{\partial r}\left(r\frac{\partial p}{\partial r}\right)+\frac{\partial^2 p}{\partial z^2}=-\frac{\omega^2}{c^2}p \tag{2.58}$$

This is once again co-ordinate separable, and so we can come up with a total solution mirroring the form we obtained in the last section (A detailed derivation is given in [18]). The range-independent solution is

$$\varphi_{RI}(r,\omega)=\frac{j}{\sqrt{8\pi r k_r(r,\omega)}}e^{j(k_r(\omega)r-\frac{\pi}{4})} \tag{2.59}$$

The WKB approximation for this case is,

$$\varphi(r_R)\backsimeq\frac{j}{\sqrt{8\pi h k_r(r_R,\omega)}}e^{+j\left(\int_{r_s'}^{r_R}k_r(r',\omega)dr'-\frac{\pi}{4}\right)} \tag{2.60}$$

where

$$k_r(r_R,\omega)=\sqrt{(\frac{\omega^2}{c^2}-(\frac{m\pi}{r_R\tan\theta})^2)} \tag{2.61}$$

and r_R is the horizontal distance from the apex to the receiver and r_S is the horizontal distance from the source to the apex.

It is clear that the environment is still 2-D in nature as evidenced by the boundary conditions in the dispersion relation. However an additional $\sqrt{r}$ is in the denominator, indicating loss due to cylindrical spreading of waves.

In an ideal world, we would be able to simulate the propagation of a wave arising out of a point source in a 3-D environment. However, it is extremely difficult to simulate such an environment, let alone extract features from it. One commonly used method is to apply separate boundary conditions and juxtapose them thereby creating a 3-D bathymetry of the environment. In order for us to understand the phenomenon of wave propagation in the ocean and hopefully negate its effects, we need to start with a simple model, which would be

the one with an infinite line source and a constant dispersion factor, and then progressively move on from there. In the next chapter we try and characterize the properties of the wave propagating in a range-dependent environment using its Wigner approximation.

2.4 CLASSIFICATION SIMULATION RESULTS

In this section, we present simulation results for the classification of two cylinders from features extracted from their propagated acoustic backscatter. The cylinder backscatters are made to propagate 4500 meters in increments of 50 meters. The wedge angles are also varied from .0625, .125 and .25 degrees respectively as shown in Figure(1). The simulations are performed for the propagated backscatter from two cylinders whose dimensions are given in Table(1). The parameters of the propagating environment are detailed in Table(2).

The spectrogram shown in Figures(2) and (3) is for the backscatter propagated up to 4500 meters in a wedge. The angle of the Wedge is .25 degrees and the distance from the apex of the wedge is arranged so that the depth of the wedge at the source is 25 meters, meaning the source was 5730 meters from the apex. . The attenuation is set to $10^{-8}m^{-1}Hz^{-1}$ to simulate realistic ocean environment. The spectrogram for the propagated backscatters from cylinders 1 and 2 is shown in Figures (2) and (3) respectively.

The ROC curves are plotted for the range independent features derived in [13]. Figure (4) Shows the comparison between central temporal moments(MOM), cepstral moments(CMOMs) and ADIMs. It can be clearly seen that the media specific ADIMs and CMOMs degrade when the wedge angle is increased this is anticipated since the environment is varied from an almost parallel-plate to a more range-dependent environment.

As it can be seen from the above results the classification performance degrades as the environment is moved away from the range-independent case. This warrants a thorough look into the equation governing the propagation model and look at the properties associated with the WKB propagation model. In Chapter 3 we investigate moments that may remain invariant to range-dependent dispersion.

Table 1: Geometry of shells

	Inner radius (m)	Outer radius (m)	h
Cylinder 1	1.19	1.20	0.83%
Cylinder 2	1.43	1.45	1.4%

Table 2: Parameters of the Propagating environment

	Water	Air	Steel
Density	1000 $\frac{kg}{m^3}$	1.2 $\frac{kg}{m^3}$	7800 $\frac{kg}{m^3}$
Speed of sound waves	1500 $\frac{m}{s}$	340 $\frac{m}{s}$	5880 (dilatational) $\frac{m}{s}$ 3140 (Shear) $\frac{m}{s}$

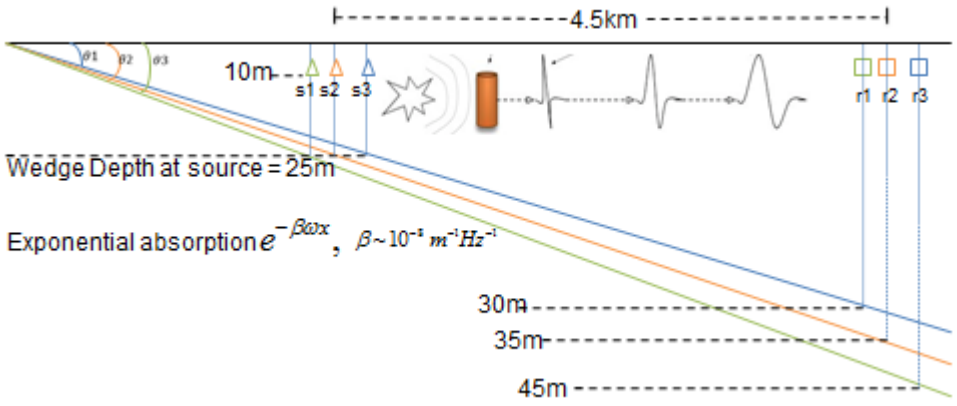

Figure 1: Wedge waveguide simulation setup

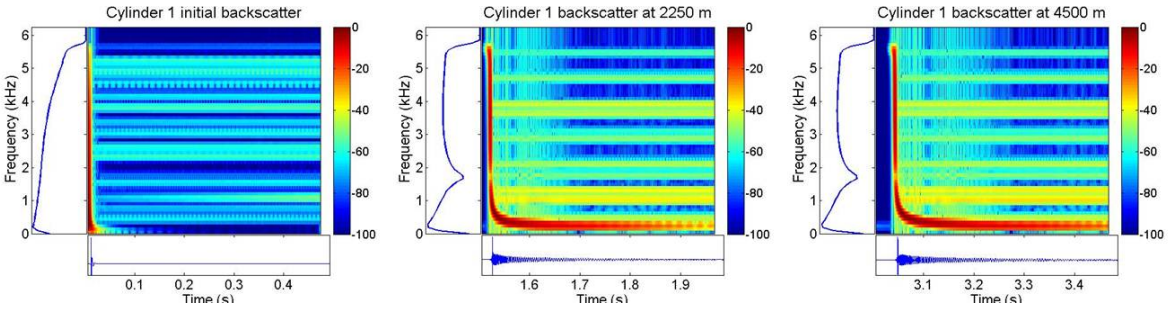

Figure 2: Backscatter plots for cylinder 1

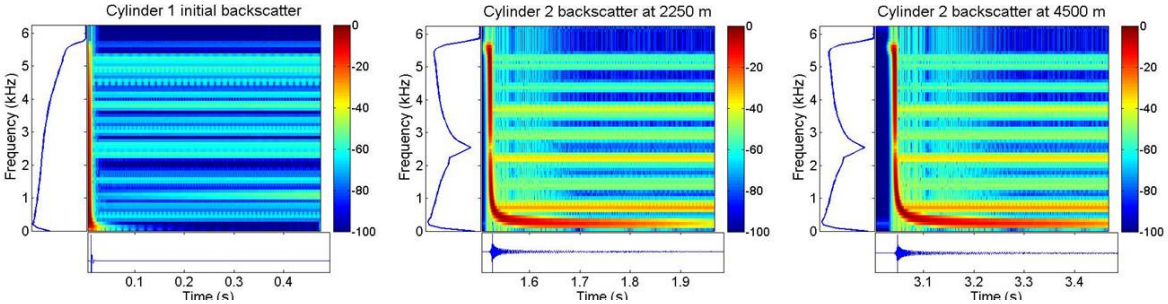

Figure 3: Backscatter plots for cylinder 2

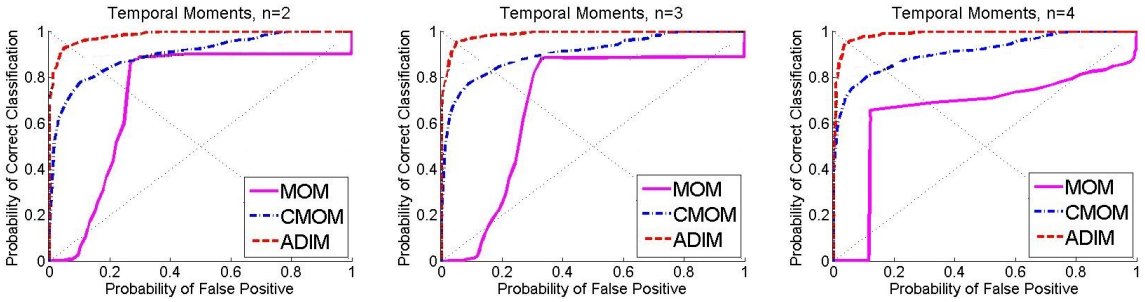

Figure 4: ROC curves of Temporal Moments wedge angle = .0625degrees

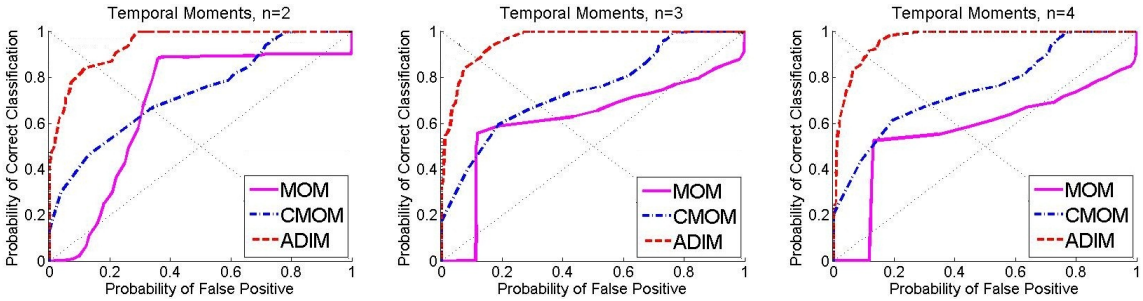

Figure 5: ROC curves of Temporal Moments wedge angle = .125degrees

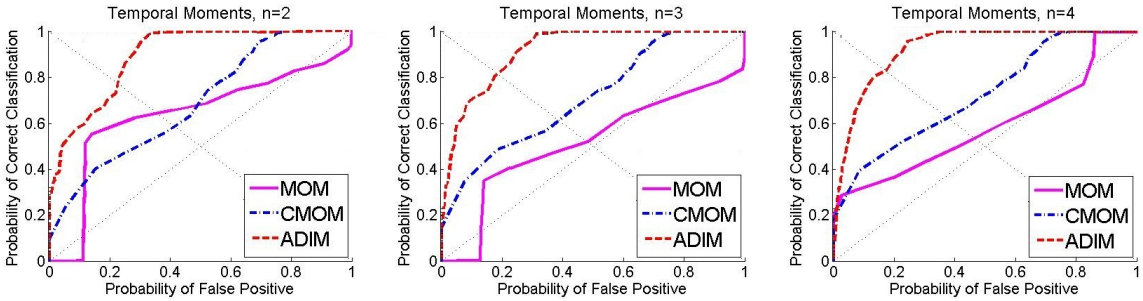

Figure 6: ROC curves of Temporal Moments wedge angle = .25degrees

3.0 WIGNER APPROXIMATION FOR RANGE DEPENDENT MEDIA

3.1 INTRODUCTION

The Wigner approximation has been used as an analytical interpretative tool for pulse propagation [9, 4]. Part of the allure lies in the ease of its application in potentially complex environments. In this chapter, we derive the Wigner approximation of the pulse propagating in an ideal wedge. We consider two cases: a line source, and a point source in a 2-D wedge.

3.2 THE WIGNER APPROXIMATION: BACKGROUND/RANGE INDEPENDENT PROPAGATION

The Wigner approximation for range-independent dispersvie pulse propagation, and for filtered signals, has been gvein in [9] and [8] respectively. In [5] it was shown that the Wigner approximations was more accurate than the stationary phase approximation. In this section we revisit the Wigner approximation for a filtered signal and extend that to the pulse propagation in a range-independent media.

The operation of linear time-invariant filter can be written as

$$y(t) = \int x(\tau)h(t-\tau)d\tau \tag{3.1}$$

where $y(t)$ is the filtered version of the signal $x(t)$ and $h(t)$ is the impulse response of the

filter. In terms of the Fourier transforms, we have

$$Y(\omega) = \int y(t)e^{-j\omega t}dt = X(\omega)H(\omega) \tag{3.2}$$

The Wigner distribution of the filtered signal is given by

$$W_y(t,\omega) = \frac{1}{2\pi}\int y(t+\frac{\tau}{2})y^*(t-\frac{\tau}{2})e^{-j\omega\tau}d\tau \tag{3.3}$$

or in the frequency domain as

$$W_y(t,\omega) = \frac{1}{2\pi}\int Y^*(\omega+\frac{\theta}{2})Y(\omega-\frac{\theta}{2})e^{-j\theta t}d\theta \tag{3.4}$$

Equivalently, the Wigner distribution of the filtered signal can be expressed as [10]

$$W_y(t,\omega) = \int W_x(t,\omega)W_h(t-\tau,\omega)d\tau \tag{3.5}$$

where

$$W_h(t,\omega) = \frac{1}{2\pi}\int H^*(\omega+\frac{\theta}{2})H(\omega-\frac{\theta}{2})e^{-j\theta t}d\theta \tag{3.6}$$

Following [8], let

$$H(\omega) = B(\omega)e^{j\psi(\omega)} = e^{\beta(\omega)+j\psi(\omega)} \tag{3.7}$$

with

$$\beta(\omega) = \ln\beta(\omega) \tag{3.8}$$

Then we have

$$W_h(t,\omega) = \frac{1}{2\pi}\int e^{\beta(\omega+\frac{\theta}{2})+\beta(\omega-\frac{\theta}{2})+j\left(\psi(\omega-\frac{\theta}{2})-\psi(\omega+\frac{\theta}{2})-\theta t\right)}d\theta \tag{3.9}$$

expanding β and ψ in a power series w.r.t θ yields [8],

$$\beta(\omega+\frac{\theta}{2})+\beta(\omega-\frac{\theta}{2}) = \sum_{n=0}^{\infty}\frac{\beta^{(2n)}(\omega)}{(2n)!}\frac{\theta^{2n}}{2^{2n-1}} = 2\beta(\omega)+\frac{1}{4}\theta^2\beta''(\omega)+\ldots \tag{3.10}$$

$$\psi(\omega - \frac{\theta}{2}) - \psi(\omega + \frac{\theta}{2}) = \sum_{n=0}^{\infty} \frac{-\psi^{(2n+1)}(\omega)}{(2n+1)!} \frac{\theta^{2n+1}}{2^{2n}} = -\theta\psi'(\omega) - \frac{1}{24}\theta^3\psi'''(\omega) + \dots \tag{3.11}$$

By a first order appoximation of Eqs. (3.10), (3.11) and subsequent plugging into Eq. (3.5) we obtain [8]:

$$W_y(t,\omega) \approx \int W_x(\tau,\omega)\,|H(\omega)|^2\,\delta(t-\tau+\psi'(\omega))d\tau \tag{3.12}$$

$$= |H(\omega)|^2\, W_x(t+\psi'(\omega),\omega) \tag{3.13}$$

The pulse propagation in a waveguide is equivalent to that of passing the signal through a filter. In particular, the pulse at x_R is related to the pulse at the source x_S by the following equation

$$F(x_R,\omega) = F(x_S,\omega)e^{jk_x(\omega)(x_R-x_S)} \tag{3.14}$$

where $F(x_S,\omega)$ is the spectrum of the pulse at the source and $h_x(\omega)$ is the dispersion relation, which has real and imaginary parts given by k_{Rx} and k_{Ix}, respectively. Then, the approximate Wigner distribution of the pulse at x_R is given by

$$W(x_R,t,\omega) \approx e^{-2k_{Ix}(\omega)(x_R-x_S)}W(x_S,t-k'_{Rx}(\omega)(x_R-x_S),\omega) \tag{3.15}$$

3.3 THE WIGNER APPROXIMATION: RANGE DEPENDENT ENVIRONMENT

In this section we derive the Wigner approximation for a wave propagating in a range dependent environment. As mentioned in the previous section, this is going to be an extension of the parallel-plate waveguide i.e. we are going to assume an infinite line source similar to the parallel plate case, so that the wave propagates in a 2-D environment. The only difference

being that the boundaries vary w.r.t range. We will also show that the Wigner approximation for a point source with azimuthal symmetry in a wedge has similar properties compared to the Wigner distribution of the propagated pulse assuming an infinite line source.

3.3.1 The Line source

To determine the Wigner approximation we need to know the impulse response of the channel. This follows from the derivation in Chapter 2.

We write the Helmholtz equation in rectangular coordinates as:

$$\frac{\partial^2 p}{\partial x^2} + \frac{\partial^2 p}{\partial z^2} = -\frac{\omega^2}{c^2} p \tag{3.16}$$

Following from the previous section we assume a solution of the form $\varphi(x) = A(x)e^{j\phi(x)}$. Subsequently, the solution is calculated to be:

$$\varphi(x_R) \backsimeq \frac{1}{\sqrt{k_x(x_R)}} e^{+j\int_{x_S}^{x_R} k_x(x')dx'} \tag{3.17}$$

The solution to a pulse propagating from source x_S to receiver x_R is given by

$$F(x_R, \omega) = F(x_S, \omega) \frac{1}{\sqrt{k_x(x_R)}} e^{j\int_{x_S}^{x_R} k_x(x')dx'} \tag{3.18}$$

where $F(x_S, \omega)$ is the Fourier transform of the pulse at source 's' and we use the positive exponent for forward propagating wave.

The Wigner distribution is given by [3],

$$W(x_R, t, \omega) = \frac{1}{2\pi} \int F^*(x_R, \omega + \frac{\lambda}{2}) F(x_R, \omega - \frac{\lambda}{2}) e^{jt\lambda} d\lambda \tag{3.19}$$

and conversely,

$$F^*(x_R, \omega + \frac{\lambda}{2}) F(x_R, \omega - \frac{\lambda}{2}) = \frac{1}{2\pi} \int W(x_R, t, \omega) e^{-jt\lambda} d\lambda \tag{3.20}$$

Using this identity, we write the Wigner distribution of the propagated pulse in terms of the Wigner of the pulse at the source,

$$W(x_R,t,\omega) = \frac{1}{2\pi}\int F(x_S,\omega-\frac{\lambda}{2})F^*(x_S,\omega+\frac{\lambda}{2})\frac{1}{\sqrt{k_x^*(x_R,\omega+\frac{\lambda}{2})k_x(x_R,\omega-\frac{\lambda}{2})}} \\ e^{-j\int_{x_S}^{x_R}k_x^*(x',\omega+\frac{\lambda}{2})dx'}e^{+j\int_{x_S}^{x_R}k_x(x',\omega-\frac{\lambda}{2})dx'} \tag{3.21}$$

writing $\int_{x_S}^{x_R} k_x(x')dx'$ as $K_x(x_R) - K_x(x_S)$ and simplification of the above term yields (See Appendix for details).

$$W(x_R,t,\omega) \approx \frac{e^{2(K_{Ix}(x_S,\omega)-K_{Ix}(x_R,\omega))}}{|k_x(x_R,\omega)|}W(x_S,t-\left[K_{Rx}^{'}(x_R,\omega)-K_{Rx}^{'}(x_S,\omega)\right],\omega) \tag{3.22}$$

Before looking at the characteristics of the Wigner approximation of the propagated pulse, it is imperative to scrutinize the propagated pulse itself. In the expression to the propagated pulse given in Eq. (3.17) the propagation effect is introduced by the exponent of the dispersion relation integrated over the distance traversed (i.e. $e^{+j\int_{x_S}^{x_R}k_x(x')dx'}$). Also there is a frequency dependent attenuation term ($\sqrt{k_x(x_R)}$) that accounts for the spreading of the wavefront in the waveguide. Using the above knowledge we can see that the approximate Wigner distribution of a propagated pulse is a frequency-dependent time-shifted version of the Wigner distribution of the original pulse, where the shifting factor is the group-delay of the waveguide. The magnitude of the dispersion relation $|k_x(x_R,\omega)|$ and the exponential attenuation $e^{2(K_{Ix}(x_S,\omega)-K_{Ix}(x_R,\omega))}$ present in Eq(3.22) is a result of bilinear transformation of the attenuation term $\sqrt{k_x(x_R)}$ present in the propagated pulse from Eq(3.17), and the imaginary part of $\int_{x_S}^{x_R} k_x(x')dx'$ in Eq(3.17) is the dispersion is complex, similar to the general expression in Eq(3.13).

Eq(3.22) can be seen as a natural progression from the range-independent propagation (considering only the dispersion part) where the total solution is of the form $e^{+jk_x(x_R-x_S)'}$,can be easily derived from Eq(3.17) if dispersion relation $k_x(x')$ is independent of x'. Consequently, the Wigner approximation is also a natural extension from the range-independent case.

3.3.2 Extension: The Point Source with Azimuthal Symmetry

An interesting observation was that the adiabatic-Mode solution also holds its validity for point sources with azimuthal symmetry in cylindrical co-ordinates which is as shown below.

Starting with the Helmholtz equation in cylindrical co-ordinates we get:

$$\frac{1}{r}\frac{\partial}{\partial x}\left(r\frac{\partial p}{\partial r}\right)+\frac{\partial^2 p}{\partial z^2}=-\frac{\omega^2}{c^2}p \tag{3.23}$$

This is once again co-ordinate separable. Hence following the steps from Chapter 2 Eq. (**??**), the total solution can be written as:

$$\varphi(r_R) \backsimeq \frac{j}{\sqrt{8\pi(r_R-r_S)k_r(r_R)}}e^{+j\left(\int_{r_S}^{r_R} k_{r_R}(r')dr'-\frac{\pi}{4}\right)} \tag{3.24}$$

We can see that the solution largely remains the same except for the $r^{\frac{1}{2}}$ term which is due to cylindrical spreading of the waves. Even though the homogeneous solution is different, the adiabatic approximate solution turns out to be similar in structure thus yielding the Wigner approximation.

Proceeding on the same vein as the previous section we obtain

$$W(x_R,t,\omega)\approx\frac{e^{2(K_{Ir}(r_S,\omega)-K_{Ir}(r_R,\omega))}}{8\pi(r_R-r_S)\left|k_r(r_R,\omega)\right|}W(r_S,t-\left[K_{Rr}^{'}(r_R,\omega)-K_{Rr}^{'}(r_S,\omega)\right],\omega) \tag{3.25}$$

This is a decisive forward step in the modeling of pulse propagation in a range-dependent media, progressing from plane wave in a fixed bounded media to a plane wave propagating in a varying media. The point source in a wedge solved here still only holds for 2-D environments and not 3-D.

The interesting fact that we learn from the Wigner approximation is that the Wigner distribution of the propagated pulse can be approximated as the Wigner of the pulse at the origin shifted in time by the derivative of the media dependent dispersion. This is validated by the fact that if the media is range independent, the Wigner approximation would be Wigner of the pulse at the source shifted in time by the product of dispersion and distance propagated.

4.0 RANGE-DEPENDENT DISPERSION INVARIANT MOMENTS

4.1 INTRODUCTION

As we have seen in Chapter 2, the features extracted for range independent propagation lose their effectiveness when applied to waves propagating in a range-dependent environment. In this chapter we consider the derivation of invariant features for classification in range-dependent environments. We compare the features obtained with the ADIMs, cepstral moments and central temporal moments, in a numerical simulation of the classification of two shells from their acoustic backscatter propagating in a wedge.

The solution to the unforced wave equation given in Eq. (4.1) is the impulse response of a weakly range dependent channel, such as the narrow wedge. Now, the backscatter propagation would be the convolution of the impulse response of the backscatter and the impulse response of the channel. The goal of this chapter would be to exploit the mathematical property of the propagated pulse and perform operations that either eliminate or neutralize the propagation effects.

4.2 FEATURE EXTRACTION

The solution to the wave equation given by Eq. (2.comsoln) is,

$$\varphi(x_R; x_S) = \frac{1}{\sqrt{k_x(x_R)}} e^{\pm j \int_{x_S}^{x_R} k_x(x')dx'} \tag{4.1}$$

using the broadband Fourier solution concept where the total solution of the propagated wave is given by the convolution of backscatter and the impulse response of propagation component. It should be mentioned that we are deriving the moments for an infinite line source in a 2-D range-dependent environment. We also restrict our derivations to a real dispersion relation (i.e. no frequency-dependent absorption).

Let $F(x_S, \omega)$ be the initial sonar backscatter from a passive object and $F(x_R, \omega)$ be the propagated backscatter response,

$$F(x_R, \omega) = \frac{F(x_S, \omega)}{\sqrt{k_x(x_R, \omega)}} e^{\pm j \int_{x_S}^{x_R} k_x(x', \omega) dx'} \tag{4.2}$$

Taking the absolute value on both sides, we have

$$|F(x_R, \omega)| = \frac{|F(x_S, \omega)|}{\sqrt{k_x(x_R)}} \tag{4.3}$$

Raise both sides to 4th power and call the function $G(''),$

$$G(x_R, \omega) = \frac{G(x_S, \omega)}{k_x^2(x_R, \omega)} \tag{4.4}$$

Substuiting from Eq. (2.36) for the dispersion relation $k_x(x_R, \omega)$ Eq. (4.4); is re-written as,

$$\left(\left(\frac{\omega}{c} \right)^2 - \left(\frac{\pi}{f(x_R)} \right)^2 \right) = \frac{G(x_S, \omega)}{G(x_R, \omega)} \tag{4.5}$$

Subtracting the mean (with respect to ω) yields,

$$\left(\left(\frac{\omega}{c} \right)^2 - \overline{\left(\frac{\omega}{c} \right)^2} \right) = \frac{G(x_S, \omega)}{G(x_R, \omega)} - \overline{\left(\frac{G(x_S, \omega)}{G(x_R, \omega)} \right)} \tag{4.6}$$

where

$$\overline{Q(\omega)} = \int Q(\omega) d\omega \tag{4.7}$$

Now, let $\widehat{G}(x_S, \omega)$ be the estimate of the source feature we are trying to recover. Rearranging Eq. (4.6) we obtain,

$$\left[\left(\left(\frac{\omega}{c} \right)^2 - \overline{\left(\frac{\omega}{c} \right)^2} \right) + \overline{\left(\frac{G(x_S, \omega)}{G(x_R, \omega)} \right)} \right] G(x_R, \omega) = \widehat{G}(x_S, \omega) \tag{4.8}$$

In this equation the information needed to perform the feature extraction are: $G(x_R, \omega)$ (computed from the received pulse) and the mean of $\frac{G(x_S,\omega)}{G(x_R,\omega)}$. If $G(x_S, \omega)$ is not known one option is to replace it with 1 and compute the mean. [1]

To compute the invariant temporal moments we first take take the inverse Fourier transform of $\widehat{G}(x_S, \omega)$

$$g(x,t) = \frac{1}{\sqrt{2\pi}} \int \widehat{G}(x_S, \omega) e^{-j\omega t} d\omega \tag{4.9}$$

The temporal feature $g(x, t)$ can now be used to compute the invariant moments

$$T_g(x; n) = \int t^n \left| g(x,t) \right|^2 dt \tag{4.10}$$

4.3 COMMENTS ON RDIMS

4.3.1 Absorption

It should be noted that the above process only works for range-dependent dispersive environment, without absorption (i.e. only real dispersion). Attempts to follow in a similar vein for an attenuating environment (i.e. complex dispersion) yielded expressions that were dis-satisfactory and unwieldy. Nevertheless, our simulations in the next section are carried out for an attenuation coefficient of $10^{-8} m^{-1} Hz^{-1}$ which is commonly found in oceanic environments.

4.3.2 Evanescent modes

At short distances for broadband pulses, the presence of evanescent modes causes the feature to under perform. The mathematical expression for the dispersion is given by

$$k_x = \sqrt{\left(\left(\frac{\omega}{c} \right)^2 - \left(\frac{m\pi}{f(x)} \right)^2 \right)} \tag{4.11}$$

[1] In a related experiment not shown here, we compared the performance of moments using both the constant and the free-field response for computing the mean. The results were nearly identical.

It can be seen that for certain low frequencies and/or short distances the dispersion relation turns imaginary causing the process to fail and subsequently degrade the classification performance. This is due to the fact that we derived the feature assuming real dispersion. Hence, the application of this feature extraction process would be limited to longer distances.

4.4 SIMULATIONS

In this section we simulate the backscatter of two cylinders propagating in a wedge up to a distance of 4500 meters, in increments of 50 meters (similar to the experiment setup in Chapter 2). The ocean environment also has an absorption co-efficient of $10^{-8}m^{-1}Hz^{-1}$. We then plot the ROC curves for all the moments (i.e. ADIMs, CMOMs, MOM and RDIMs). We repeat the experiment for wedge angles of .0625, .125 and .25 degrees respectively to analyze the behavior of the invariant moments with changing environment.

Figures (7), (8) and (9) show the simulation results comparing the classification performance of ADIMs, CMOMs and MOMs with RDIMs. It is plainly visible from the ROC curves that as the wedge angle increases (environment changes from a nearly parallel two-plate to a more range-dependent form), the range-independent moments degrade while the RDIMs offer robust performance despite the change.

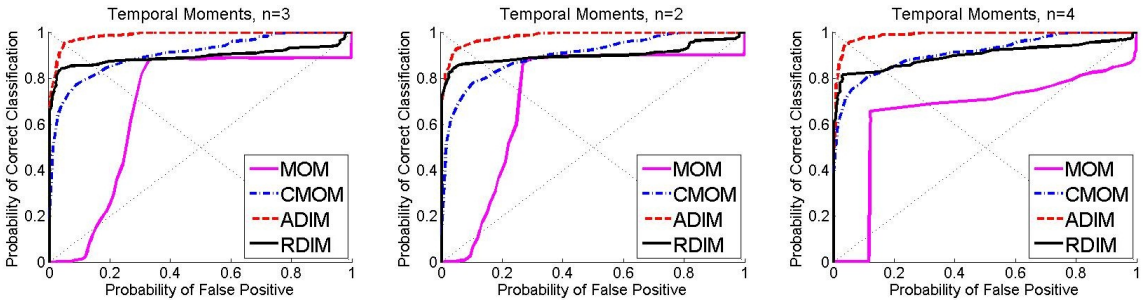

Figure 7: ROC curves of Temporal Moments wedge angle = .0625degrees

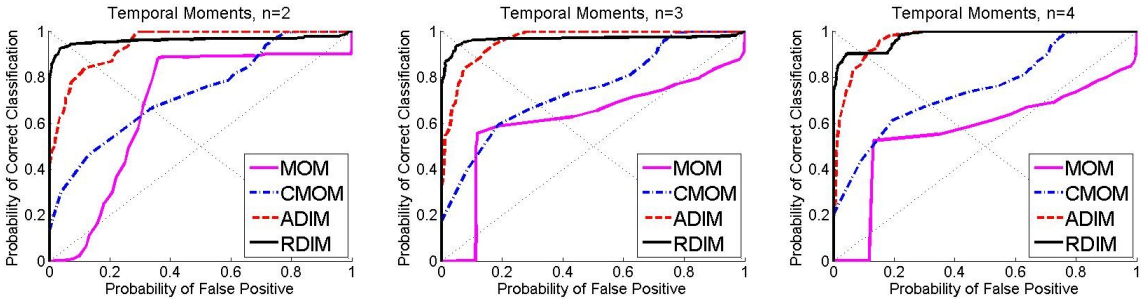

Figure 8: ROC curves of Temporal Moments wedge angle = .125degrees

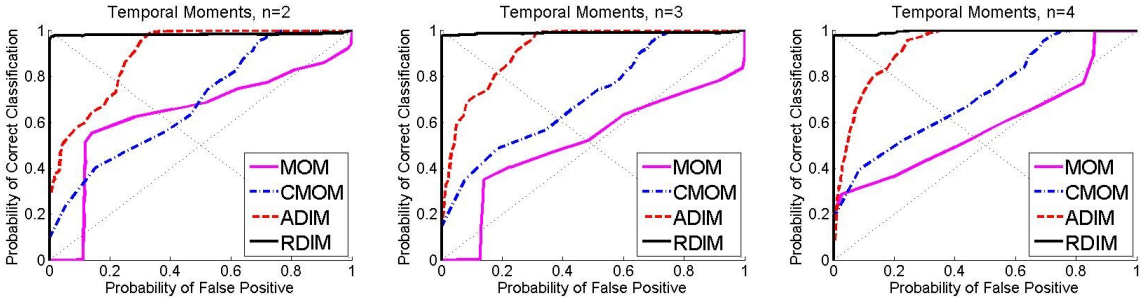

Figure 9: ROC curves of Temporal Moments wedge angle = .25degrees

5.0 THE PARABOLIC EQUATION (PE) MODEL

5.1 INTRODUCTION

The Parabolic Equation (PE) approximation was first adapted to underwater acoustics by Hardin and Tappert[7] and they devised an efficient numerical algorithm scheme to solve the parabolic equation using Fourier transforms. In the past decade and a half, the interest on the PE has skyrocketed as evidenced by the drastic increase in the number of publications over that duration. The reason behind the widespread interest in PE lies in the fact that a variety of complex environments with complex bottom interactions can be modeled without any significant variations in the initial problem formulation or the computation time. Deservedly, the PE is the most widely used method to solve and model the range-dependent propagation problems in ocean acoustics.

If we are able to extract features for pulse propagation in this model, we could potentially extract invariant features in the real world using the same algorithm developed for the PE model, since this model can be used to simulate pulse propagation in a variety of environments with high degree of accuracy. This would also, to a large degree, address the major issues in object classification using feature extraction in underwater acoustics. In subsequent sections, we will first detail the construction of the parabolic model and the procedure for evaluating the field of the propagated wave. We will show that there are mathematically tractable methods which can (in theory) extract features that are invariant to dispersion and different forms of attenuation. This feature extraction process also requires less processing compared to the process discussed in Chapter 4.

5.2 THE PARABOLIC EQUATION

We derive the solution for the 2-D fluid environment starting from the Helmholtz equation for a uniform medium in cylindrical co-ordinates (r, θ, z), given by

$$\frac{\partial^2 p}{\partial r^2} + \frac{1}{r}\frac{\partial p}{\partial r} + \frac{1}{r^2}\frac{\partial^2 p}{\partial \theta^2} + \frac{\partial^2 p}{\partial z^2} + k_0^2 n^2 p = 0 \tag{5.1}$$

In subsequent equations θ as it is neglected due to cylindrical symmetry, following Tappert [15], we assume the solution of the form

$$p(r, z) = \psi(r, z; \omega) H_0^{(1)}(k_0 r; \omega) \tag{5.2}$$

Ofcourse a solution of this form is possible only when we assume exponential time dependence for the wave. k_0 is the reference wavenumber (i.e. wavenumber of air media), r is the range component, z is the depth component, n is the refractive index of the media. We omit the ω henceforth, since that is the domain that we operate on.

The purpose of assuming the solution of this form is that it is conveniently split into two components: the dispersion-free propagating component in the form of an outgoing Hankel function and the range-depndent dispersive envelope $\psi(r, z; \omega)$ whose solution needs to be ascertained.

5.2.1 Derivation of the Parabolic Equation PE in standard form

We now solve for the range-dependent-dispersive envelope. This is made mathematically simple to solve (detailed in section (2.2)) by using the narrow angle approximation of the range-dependent field.

We first substitute the solution Eq(5.2) into Eq(5.1) which yields

$$\frac{\partial^2 \psi}{\partial r^2} + \left(\frac{2}{H_0^{(1)}(k_0 r)} \frac{\partial H_0^{(1)}(k_0 r)}{\partial r} + \frac{1}{r} \right) \frac{\partial \psi}{\partial r} + \frac{\partial^2 \psi}{\partial z^2} + k_0^2 (n^2 - 1)\psi = 0 \tag{5.3}$$

and

$$\frac{\partial^2 H_0^{(1)}(k_0 r)}{\partial r^2} + \frac{1}{r}\frac{\partial H_0^{(1)}(k_0 r)}{\partial r} + k_0^2 H_0^{(1)}(k_0 r) = 0 \tag{5.4}$$

holds, as Hankel function is a solution to the Bessel differential equation. Now, back substituting Eq(5.3) to Eq(5.4) and using the asymptotic approximation for the Hankel function [20]

$$H_0^{(1)}(k_0 r) \backsimeq \sqrt{\frac{2}{\pi k_0 r}} e^{j(k_0 r - \frac{\pi}{4})} \tag{5.5}$$

we obtain,

$$\frac{\partial^2 \psi}{\partial r^2} + 2ik_0 \frac{\partial \psi}{\partial r} + \frac{\partial^2 \psi}{\partial z^2} + k_0^2(n^2 - 1)\psi = 0 \tag{5.6}$$

Using the paraxial approximation, we neglect the highest order range term in Eq(5.6) i.e.

$$\frac{\partial^2 \psi}{\partial r^2} \ll 2ik_0 \frac{\partial \psi}{\partial r} \tag{5.7}$$

yielding,

$$2ik_0 \frac{\partial \psi}{\partial r} + \frac{\partial^2 \psi}{\partial z^2} + k_0^2(n^2 - 1)\psi = 0 \tag{5.8}$$

This is the standard form of the parabolic equation derived by Tappert [15]. This form will be used in the range-marching solution that is discussed in the next section. Some of the major advantages in using range-marching solution are: The errors due to approximation tend to converge , easy computation and less memory requirement.

5.2.2 The Split-Step Fourier algorithm

The narrow angle approximation performed in Eq((5.7)) is convenient for the range-marching solution approach, elaborated in this section, using the Split-Step Fourier (SSPE) method suggested by Tappert et.al in [7]. This stems from Eq(5.8) where a spatial transfrom in $z \rightarrow k_z$ yields,

$$2ik_0 \frac{\partial \psi(r, k_z)}{\partial r} - k_z^2 \psi(r, k_z) + k_0^2(n^2 - 1)\psi(r, k_z) = 0 \tag{5.9}$$

Rearranging this equation gives,

$$\frac{\partial\psi(r,k_z)}{\partial r}+\frac{k_0^2(n^2-1)-k_z^2}{2ik_0}\psi(r,k_z)=0 \tag{5.10}$$

whose solution is given by,

$$\psi(r,k_z)=\psi(r_0,k_z)e^{-\frac{k_0^2(n^2-1)-k_z^2}{2ik_0}(r-r_0)} \tag{5.11}$$

The term $\psi(r_0,k_z)$ is the initial value condition. For the range-marching solution method, $\psi(r_0,k_z)$ is the solution of the previous step and $r-r_0=\triangle r$ is the range step size.

In order to iteratively solve for the field we need a starting point. A variety of starter fields have been proposed, the most straightforward one would be the Normal-Mode starter which is given by,

$$\psi(0,z)=\frac{\sqrt{2\pi}}{\rho(z_s)}\frac{\psi(z_s)\psi(z)}{\sqrt{k_r}} \tag{5.12}$$

A short introduction on the various starter fields is given in section(5.2.3).

The split-step fourier transform is performed by taking Eq. (5.11) and performing an inverse spatial Fourier transform to obtain

$$\psi(r,z)=e^{\frac{ik_0(n^2-1)}{2}(r-r_0)}\int_{-\infty}^{\infty}\psi(r_0,k_z)e^{-\frac{ik_z^2}{2k_0}(r-r_0)}e^{ik_zz}dk_z \tag{5.13}$$

writing $r-r_0=\triangle r$, the split-step is finally written as,

$$\psi(r,z)=e^{\frac{ik_0(n^2-1)}{2}\triangle r}F^{-1}\left\{e^{-\frac{ik_z^2}{2k_0}\triangle r}F\left\{\psi(r_0,z)\right\}\right\} \tag{5.14}$$

It should be noted that even though the refractive index n is both range and depth dependent, it is treated as a constant while computing Fourier transforms. However, it has been shown in [7] that the error is of small order (i.e. the order of the step-size).

5.2.3 Starter Fields

It has been shown in Eq. (5.14) that the field at r is a function of the field at the previous range point r_0 and the propagation effects induced in the range-step. As mentioned before there needs to be a starting field from which the field can be propagated to any desired point, changing the boundary conditions in accordance at each range step $\triangle r$.

For our feature extraction process it is of peripheral importance as to what type of starter field is used. But, for the sake of completeness, we will mention a couple of widely used starter fields. For more details the reader is referred to [18, 15, 16].

5.2.3.1 The Modal Starter The starting field for mode m=1 is given by

$$\psi(0,z) = \frac{\sqrt{2\pi}}{\rho(z_s)} \frac{sin\left(\frac{\pi}{z_s}\right) sin\left(\frac{\pi}{z}\right)}{\sqrt{k_r}} \tag{5.15}$$

z_s is the depth at which the source is placed and z is the depth of the waveguide at the point where the source is placed, $k_r = \sqrt{\left(\frac{\omega}{c}\right)^2 - \left(\frac{\pi}{z}\right)^2}$ is the dispersion relation at the source, and $\rho(z_s)$ is the source density which for all practical purposes can be assumed to be a constant.

However, this starter field suffers from the narrow angle approximation error. Namely, the source is directive in nature, so to accurately asses the field at the receiver, the receiver should be at a considerable distance from the source [**?**].

The modal starter is also particularly useful while benchmarking the PE solution to the normal mode in simpler environments, since the starter field is similar to that of Normal-mode solution.

5.2.3.2 The Gaussian Starter The Gaussian starter belongs to the class of analytical starters. These are designed to match the farfield result of the point-source solution of the Helmholtz equation in a homogeneus medium. The Gaussian starter is the most widely used starter fields in practical simulations. This is mainly due to the fact that the beamwidth, directivity and peak power can be easily adjusted while changing only a few parameters.

The starting function is of the form

$$\psi(0,z) = Ae^{-\frac{(z-z_s)^2}{W^2}} \tag{5.16}$$

where A is the height at which the source is placed and W is the beamwidth of the transmitting source.

Upon comparing the above starting function to the SSPE solution form given in Eq. (5.14), we get

$$\psi(0,z) = \sqrt{k_0}e^{-\frac{k_0^2(z-z_s)^2}{2}} \tag{5.17}$$

where $k_0 = \frac{\omega}{c_0}$ and c_0 is the sound speed in air.

It is important to mention here that we have omitted a significant amount of steps to arrive at the solution. This is due to aforementioned fact that this is only tangential to the discussion that is to follow. The reader is referred to [18, 15].

5.2.4 Attenuation Factor

The wave undergoes attenuation (i.e. frequency-dependent absorption) when the wave number(or its co-ordinate component) is complex in nature. Hence, the attenuation can be simulated by adding an imaginary part to the wavenumber term, this is analogus to what we did in the normal-mode and adiabatic-mode models except the dispersion relation was complex in those cases.

$$k = \frac{\omega}{c} + i\alpha \tag{5.18}$$

This is added as a complex term in the refractive index

$$n^2 = \left(\frac{k}{k_0}\right)^2 \backsimeq \left(\frac{c_0}{c}\right)^2 \left[1 + i\frac{2\alpha c}{\omega}\right] \tag{5.19}$$

where $k_0 = \frac{\omega}{c_0}$ is the wavenumber in air (i.e. reference wavenumber) and $k = \frac{\omega}{c}$ is the wavenumber in the medium.

Eq. (5.11) becomes,

$$\psi(r,k_z)=\psi(r_0,k_z)e^{-\frac{k_0^2\left(\left(\frac{c_0}{c}\right)^2\left[1+i\frac{2\alpha c}{\omega}\right]-1\right)-k_z^2}{2ik_0}(r-r_0)} \tag{5.20}$$

The above equation is the solution for one range-step with attenuation at that particular step.

5.3 THE FEATURE EXTRACTION PROCESS

The objective of feature extraction process is to remove propagation effects caused by the environment, from the received sound field. In the parabolic model this would be the $\psi(r,z)$ term that is causing it. Upon closer inspection of Eq. (5.11) and its modified form Eq. (5.20) we conclude that the exponential term adds dispersion and attenuation at each iteration.

Rewriting Eq(5.20), for each step $r-r_0$ we have

$$\psi(r,k_z)=\psi(r_0,k_z)e^{i\left[\frac{k_0\left(\left(\frac{c_0}{c}\right)^2-1\right)}{2}-\frac{k_z^2}{2k_0}\right](r-r_0)}e^{-k_0\left(\left(\frac{c_0}{c}\right)^2\left[\frac{\alpha c}{\omega}\right]\right)(r-r_0)} \tag{5.21}$$

However, assuming uniform media (i.e. at each range step the medium properties and the boundaries are identical) there are N steps from source at 0 to the receiver at r and that $\triangle r=(r-r_0)=r/N$ we can proceed as,

$$\psi(r,k_z)=\psi(0,k_z)e^{i\left[\frac{k_0\left(\left(\frac{c_0}{c}\right)^2-1\right)}{2}-\frac{k_z^2}{2k_0}\right]\triangle rN}e^{-k_0\left(\left(\frac{c_0}{c}\right)^2\left[\frac{\alpha c}{\omega}\right]\right)\triangle rN} \tag{5.22}$$

With little modification, the above equation holds for nonuniform and complex media (i.e. for varying k_z, c and α at each interval $\triangle r$) as N in the exponent will be replaced by a summation of N intervals representing N segments from the source to the receiver. i.e.

$$\psi(r,k_z)=\psi(0,k_z)e^{i\left\{\sum_{i=1}^{N}\left[\frac{k_0\left(\left(\frac{c_0}{c_i}\right)^2-1\right)}{2}-\frac{k_{zi}^2}{2k_0}\right]\right\}\triangle r}e^{-k_0\left\{\sum_{i=1}^{N}\left(\left(\frac{c_0}{c_i}\right)^2\left[\frac{\alpha_i c_i}{\omega}\right]\right)\right\}\triangle r} \tag{5.23}$$

However, the feature extraction process that is to follow will hold for Eq. (5.23)

In order to get rid of both exponential terms (and thereby the propagation effects) the following needs to be done. First, we take the absolute value of Eq. (5.23) which would eliminate the complex exponent. Then we have one exponent term remaining. The remaining exponent term is independent of frequency if the attenuation is not dependent on frequency. But, for SONAR propagation in underwater ocean the attenuation is indeed dependent on frequency and is written as $\alpha = \beta\omega$, where β is media dependent attenuating factor and is $10^{-8} Hz^{-1} m^{-1}$ for most oceanic environments.

Hence, we rewrite Eq. (5.23) as

$$|\psi(r, k_z; \omega)| = \left| \psi(0, k_z; \omega) e^{-k_0 \left(\left(\frac{c_0}{c} \right)^2 \left[\frac{\beta \omega c}{\omega} \right] \right) \triangle r N} \right| \tag{5.24}$$

or

$$|\psi(r, k_z; \omega)| = \left| \psi(0, k_z; \omega) e^{-\omega n \beta \triangle r N} \right| \tag{5.25}$$

natural log on both sides yields,

$$\ln |\psi(r, k_z; \omega)| = \ln |\psi(0, k_z; \omega)| - \omega n \beta \triangle r N \tag{5.26}$$

differentiation w.r.t. ω gives,

$$\frac{\partial \ln |\psi(r, k_z; \omega)|}{\partial \omega} = \frac{\partial \ln |\psi(0, k_z; \omega)|}{\partial \omega} - n \beta \triangle r N \tag{5.27}$$

the level shift can be eliminated by subtracting the mean of feature over ω .

Let,

$$\frac{\partial \ln |\psi(r, k_z; \omega)|}{\partial \omega} = Z(r, k_z; \omega) \tag{5.28}$$

$$\frac{\partial \ ln |\psi(0, k_z; \omega)|}{\partial \omega} = Z(0, k_z; \omega) \tag{5.29}$$

we obtain,

$$Z_0(0, k_z; \omega) = Z(r, k_z; \omega) - \overline{Z(r, k_z; \omega)} \tag{5.30}$$

where

$$\overline{Z(x,\omega)} = \int Z(x,\omega)d\omega \tag{5.31}$$

It is evident from Eq. (5.30) that we are able to obtain a feature from the channel model that is constant irrespective of the propagated distance. We can therefore apply this extraction process on the propagated signal to get a feature that is invariant to the propagation effects.

However, application of this in the real world would be an interesting conundrum. Since the majority of extraction process is done in the $k_z$domain, we would need the entire depth profile of the received signal. This would be a laborious task in practice. One of the possible solutions would be to have multiple microphone receivers across the depth of the ocean separated at the spatial Nyquist rate.

6.0 CONCLUSIONS AND FUTURE DIRECTIONS

In this work we built upon previously developed propagatio-invariant moment features for range-independent environments, by developing methods for range-dependent models. We were able to show that the range-dependent invariant moments (RDIMs) showed satisfactory classification performance and outperformed previously derived invariant features. This despite the fact that we derived moments assuming a purely dispersive media, and our simulations tried to mimic the ocean environment by adding ambient noise and absorption.

We also studied the characteristics of the range-dependent propagation and derived the Wigner approximation for it. The Wigner approximation remained similar to the one derived for range-independent propagation in that the approximate Wigner distribution of the propagated pulse is the frequency-dependent time-shifted version of the Wigner distribution of the initial pulse. The time-shift is dictated by the dispersion factor induced by the propagating media and the distance traversed by the pulse.

We then explored the possibility of using the parabolic model for propagation and subsequently try and extract invariant moments from it. We showed that it is mathematically tractable to extract features that are invariant to both dispersion and attenuation from the way the model is structured. This is an interesting area to pursure because parabolic models are the most widely used propagation model and it has been shown that they do indeed produce accurate results compared to that of a real propagation environment. Features derived using a model that mimics the physical environment implies that the features could be used in the real world with high degree of accuracy.

An immediate work to pursure would be to simulate the extracted features for the parabolic model and measure the classification performance of the extracted feature.

Another worthy future direction would be to use the information obtained from the

computation of the Wigner approximation and design Time-Frequency distribution kernels that could possibly negate the propagation effects induced by the channel thereby providing better object resolution. This could be used in conjunction to the works by Atlas [2] who designed TFD kernels that maximizes classfication performance.

APPENDIX

THE WIGNER APPROXIMATION SIMPLIFICATION

The Wigner distribution of the propagated pulse at h in terms of the Wigner distribution of the initial pulse at s is written as [9]

$$W(x_R,t,\omega) = \iint W(x_S,t',\omega) \frac{e^{-j(K_x^*(x_R,\omega+\lambda/2)-K_x^*(x_S,\omega+\lambda/2))}e^{+j(K_x(x_R,\omega-\lambda/2)-K_x(x_S,\omega-\lambda/2))}e^{j\lambda(t-t')}}{\sqrt{k_x^*(x_R,\omega+\lambda/2)k_x(x_R,\omega-\lambda/2)}}d\lambda dt' \quad (.1)$$

The dispersion relation can be split into real and imaginary parts.

$$k_{xn}(\omega) = k_{Rxn}(\omega) + jk_{Ixn}(\omega)K_{xn}(\omega) = K_{Rxn}(\omega) + jK_{Ixn}(\omega) \quad (.2)$$

and

$$K_{xn}(\omega) = K_{Rxn}(\omega) + jK_{Ixn}(\omega) \quad (.3)$$

where

$$K_{xn}(\omega) = K_{Rxn}(\omega) + jK_{Ixn}(\omega) \quad (.4)$$

and

$$K_{xn}(x_R,\omega) - K_{xn}(x_S,\omega) = \int_{x_S}^{x_R} k_{xn}(x',\omega)dx' \quad (.5)$$

for mode n. However, without loss of generality, we can extend this to any mode. Thus we drop the subscript n from here on.

The Taylor series expansion is given by [12].

$$K_{Ix}(\omega-\frac{\lambda}{2})+K_{Ix}(\omega+\frac{\lambda}{2})=\sum_{n=0}^{\infty}\frac{K_{Ix}^{(2n)}(\omega)}{2n!}\frac{\lambda^{2n}}{2^{2n-1}}\approx 2K_{Ix}(\omega)+\frac{1}{4}K_{Ix}^{''}(\omega)\lambda^2 \tag{.6}$$

$$K_{Rx}(\omega-\frac{\lambda}{2})-K_{Rx}(\omega+\frac{\lambda}{2})=\sum_{n=0}^{\infty}\frac{K_{Rx}^{(2n+1)}(\omega)}{2n+1!}\frac{\lambda^{2n+1}}{2^{2n}}\approx K_{Rx}^{'}(\omega)\lambda+\frac{1}{24}K_{Rx}^{'''}(\omega)\lambda^3 \tag{.7}$$

The product in the denominator of Eq. (.1) is written as

$$\begin{aligned}&\left(k_{Rx}(\omega+\frac{\lambda}{2})-jk_{Ix}(\omega+\frac{\lambda}{2})\right)\left(k_{Rx}(\omega-\frac{\lambda}{2})+jk_{Ix}(\omega-\frac{\lambda}{2})\right)=\\&k_{Rx}(\omega-\frac{\lambda}{2})k_{Rx}(\omega+\frac{\lambda}{2})+k_{Ix}(\omega-\frac{\lambda}{2})k_{Ix}(\omega+\frac{\lambda}{2})+jk_{Ix}(\omega-\frac{\lambda}{2})k_{Rx}(\omega+\frac{\lambda}{2})(-)\\&(-)jk_{Rx}(\omega-\frac{\lambda}{2})k_{Ix}(\omega+\frac{\lambda}{2})\end{aligned} \tag{.8}$$

Expanding the terms into Taylor series of order 2:

$$k_{Rx}(\omega-\frac{\lambda}{2})k_{Rx}(\omega+\frac{\lambda}{2})=(k_{Rx}(\omega))^2+\left(k_{Rx}^{'}(\omega)\frac{\lambda}{2}\right)^2 \tag{.9}$$

$$k_{Ix}(\omega-\frac{\lambda}{2})k_{Ix}(\omega+\frac{\lambda}{2})=(k_{Ix}(\omega))^2+\left(k_{Ix}^{'}(\omega)\frac{\lambda}{2}\right)^2 \tag{.10}$$

$$\begin{aligned}jk_{Ix}(\omega-\frac{\lambda}{2})k_{Rx}(\omega+\frac{\lambda}{2}) &= jk_{Ix}(\omega)k_{Rx}(\omega)-jk_{Ix}^{'}(\omega)k_{Rx}(\omega)\frac{\lambda}{2}(+)\\&\quad (+)jk_{Ix}^{'}(\omega)k_{Rx}(\omega)\frac{\lambda}{2}-jk_{Ix}^{'}(\omega)k_{Rx}^{'}(\omega)\left(\frac{\lambda}{2}\right)^2\end{aligned} \tag{.11}$$

$$\begin{aligned}jk_{Rx}(\omega-\frac{\lambda}{2})k_{Ix}(\omega+\frac{\lambda}{2}) &= jk_{Rx}(\omega)k_{Ix}(\omega)-jk_{Rx}^{'}(\omega)k_{Ix}(\omega)\frac{\lambda}{2}(+)\\&\quad (+)jk_{Rx}^{'}(\omega)k_{Ix}(\omega)\frac{\lambda}{2}-jk_{Rx}^{'}(\omega)k_{Ix}^{'}(\omega)\left(\frac{\lambda}{2}\right)^2\end{aligned} \tag{.12}$$

Keeping only the first order terms we get:

$$\left(k_{Rx}(\omega+\frac{\lambda}{2})-jk_{Ix}(\omega+\frac{\lambda}{2})\right)\left(k_{Rx}(\omega-\frac{\lambda}{2})+jk_{Ix}(\omega-\frac{\lambda}{2})\right)\approx\left(k_{Rx}(\omega)\right)^2+\left(k_{Ix}(\omega)\right)^2 \quad (.13)$$

Splitting K and k into real and imaginary parts as mentioned before and using the Taylor Series approximation shown here, we can reduce the equation to

$$W(x_R,t,\omega)\approx e^{2(K_{Ix}(x_S,\omega)-K_{Ix}(x_R,\omega))}\iint\frac{e^{-j\lambda(K^{'}_{Rx}(x_R,\omega)-K^{'}_{Rx}(x_S,\omega))}e^{j\lambda(t-t')}}{\sqrt{k^2_{Rx}(x_R,\omega)+k^2_{Ix}(x_R,\omega)}}W(x_S,t',\omega)d\lambda dt' \quad (.14)$$

$$W(x_R,t,\omega)\approx\frac{e^{2(K_{Ix}(x_S,\omega)-K_{Ix}(x_R,\omega))}}{|k(x_R,\omega)|}W(x_S,t-\left[K^{'}_{Rx}(x_R,\omega)-K^{'}_{Rx}(x_S,\omega)\right],\omega) \quad (.15)$$

BIBLIOGRAPHY

[1] O. Aluko. Implementation and application of dispersion-based waveguide models for shallow-water sonar processing. Master's thesis, University of Pittsburgh, 2003.

[2] L. Atlas, J. Droppo, and J. McLaughlin. Optimizing time-frequency distributions for automatic classification. In *Proc. SPIE*, volume 3162, pages 161–171. Citeseer, 1997.

[3] L. Cohen. *Time-Frequency Analysis*. Prentice Hall Signal Processing Series. Prentice Hall, 1995.

[4] L. Cohen. The wigner distribution and pulse propagation. In *SPIE proceedings series*, pages 20–24. Society of Photo-Optical Instrumentation Engineers, 2001.

[5] L. Cohen, P. Loughlin, and G. Okopal. Exact and approximate moments of a propagating pulse. *Journal of Modern Optics*, 55(19):3349–3358, 2008.

[6] L. B. Felsen and N. Marcuvitz. *Radiation and Scattering of Waves*. IEEE Press Series on Electromagnetic Wave Theory, 1973.

[7] RH Hardin and FD Tappert. Applications of the split-step fourier method to the numerical solution of nonlinear and variable coefficient wave equations. *Siam Rev*, 15:423, 1973.

[8] P. Loughlin. Time-varying spectral approximation of filtered signals. *Signal Processing Letters, IEEE*, 13(10):604–607, 2006.

[9] P. Loughlin and L. Cohen. A wigner approximation method for wave propagation. *The Journal of the Acoustical Society of America*, 118(3):1268–1271, 2005.

[10] W.D. Mark. Spectral analysis of the convolution and filtering of non-stationary stochastic processes. *Journal of Sound and Vibration*, 11(1):19–63, 1970.

[11] G. Okopal. Implementation and evaluation of dispersion-invariant features for signal classification. Master's thesis, University of Pittsburgh, 2007.

[12] G. Okopal. *Phase space analysis and classification of sonar echoes in shallow-water channels*. PhD thesis, University of Pittsburgh, 2009.

[13] G. Okopal and P.J. Loughlin. Propagation-invariant classification of sounds in channels with dispersion and absorption. *The Journal of the Acoustical Society of America*, 128:2888, 2010.

[14] G. Okopal, P.J. Loughlin, and L. Cohen. Dispersion-invariant features for classification. *The Journal of the Acoustical Society of America*, 123:832, 2008.

[15] F. Tappert. The parabolic approximation method. *Wave propagation and underwater acoustics*, pages 224–287, 1977.

[16] CT Tindle, H. Hobaek, and TG Muir. Normal mode filtering for downslope propagation in a shallow water wedge. *The Journal of the Acoustical Society of America*, 81:287–294, 1987.

[17] I. Tolstoy and C. S. Clay. *Ocean Acoustics : Theory and Experiment in Underwater Sound*. Acoustical Society of America, 1987.

[18] M.B.Porter H.Schmidt W.A.Kuperman, F.B.Jensen. *Computational ocean acoustics*. Amer Inst of Physics, 1994.

[19] H. Weinberg and R. Burridge. Horizontal ray theory for ocean acoustics. *The Journal of the Acoustical Society of America*, 55:63–79, 1974.

[20] G. B. Whitham. *Linear and Nonlinear Waves (Pure and Applied Mathematics)*. Wiley-Interscience, 1974.